CERN–ACC–NOTE–2022–XXXX

March 28, 2022

arek.gorzawski@cern.ch

Determination of BLM conversion factors for collimators scans

A. Gorzawski, M. Giovannozzi

Keywords: LHC, collimator scan, beam halo, beam losses

Summary

This note summarises the results of a study related to a method used to obtain the conversion factor to calibrate in protons/s the signals measured in Gy/s by the BLM system during the collimator scans. Data and analysis presented here are based on the work carried out on the beam-halo reconstruction during beam tail scraping measurements performed in the LHC Run 2.

1 Introduction and data analysis principle

The LHC beam loss monitors (BLMs) system provides the beam loss measurement expressed in Gy/s. These values can be obtained for different integration times, so-called Running Sums (RS) [1, 2]. However, many simulations and modelling tools are based on the use of losses expressed as protons/s, therefore it is essential to provide a reliable means to convert the measured values into a quantity that can be used in numerical simulations. The LHC collimation system is set up to protect the ring, and to achieve this purpose, all betatron losses are caught by the collimators located in IR7. Therefore, using the BLMs in IR7, it is possible to calibrate the BLM signal at selected locations to achieve a direct measurement in terms of protons/s

During the LHC Run 2, many experiments on beam tail reconstruction were carried out using collimator scans, which were performed between 2016 and 2018 [3]. Probing the beam distribution with small steps in the position of the collimator's jaws allows loss patterns to be created. The absolute value of protons scraped by the collimator step is measured simultaneously by means of the DC beam current transformer (BCTDC). To calibrate the BLM signals, due to a limited resolution of the beam intensity measurement performed by the BCTDC, an intermediate step is required to convert high-resolution loss data from BLMs using sparse BCTDC data. This step consists of comparing all relevant loss processes to the total intensity lost on a longer period of time.

2 Experiment and data source

Figure 1 shows the loss evolution during one of the collimator scans. One can notice that along the process, when a collimator jaw is gradually inserted in steps towards the beam core, the overall loss level increases.

Figure 2 shows the evolution of beam loss during the experiment carried out using the three primary collimators installed in the betatron cleaning insertion, namely, horizontal, vertical, and skew collimator. During individual steps, more distinct loss peaks can be identified. Last but not least, the

individual spikes (see the example in Fig. 3) represent a BLM response for each collimator step. It consists of fast raise and subsequent exponential decay, during which the diffusion process approaches an equilibrium. In the same figure, one can also see the associated beam intensity lost during that step.

Figures 1 to 3 refer to the LHC fill 6052, whereas the following discussion refers to more fills performed during the LHC Run 2 (for more details on the fills, see Table 2 in the Appendix A).

In the analysis described in the following, we treated each step and spike within one collimator scan experiment and computed the conversion factor w.r.t. the jaw position during the scraping. All the data used for the computations reported in this note are stored in the CERN accelerator logging system (CALS) [4]. Unfortunately, due to the huge storage capacity needed for the high acquisition rate data, e.g. RS06 at 100 Hz, the data older than half a year are compressed and only accessible as 1 Hz data. However, for collimator alignment [5], the high acquisition rate data is retained in the dedicated storage on the NFS [6] file system. The subsequent analysis combines both data sources. In Appendix B we show the impact (lack of it) of usage of different running sums on the loss integrals we use later in the analysis (see Sec. 3).

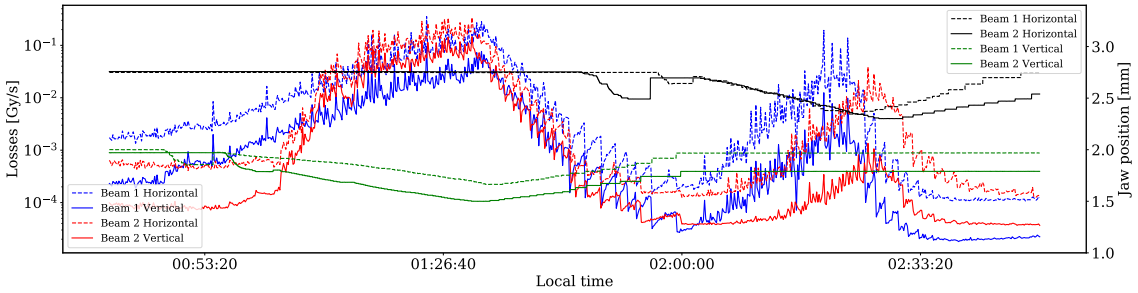

Figure 1: Beam losses from the BLM monitor during LHC fill 6052. Beam 1 and Beam 2 data are shown (blue and red, respectively), together with the positions of the collimator's jaws (black and green, respectively). Scraping is performed first in the vertical plane for both beams simultaneously. Afterwards, the scraping is performed in the horizontal plane.

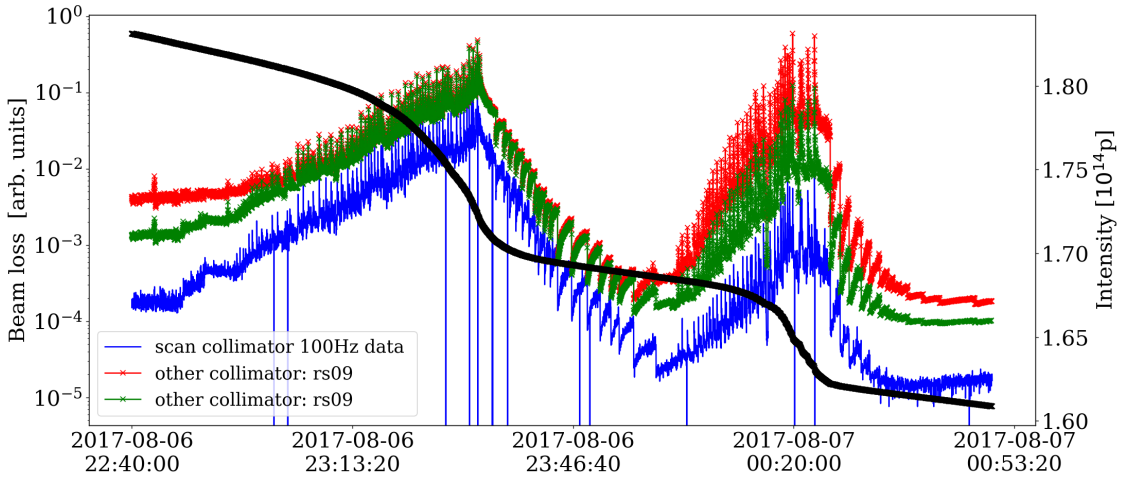

Figure 2: Overview of the beam losses recorded by the three primary collimators: vertical (blue), horizontal (red) and skew (green) during the collimator scan experiment in LHC fill 6052. In black, the BCTDC intensity evolution during the beam measurements.

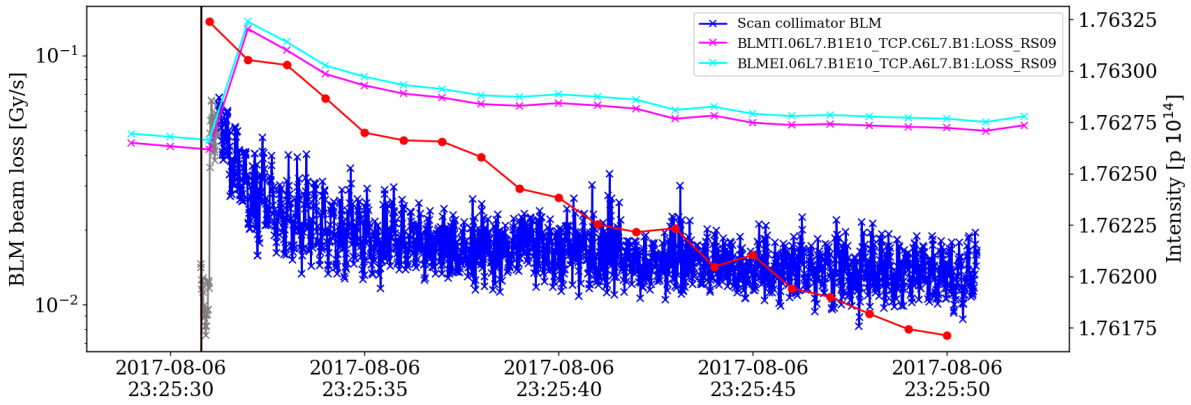

(a) Inward step

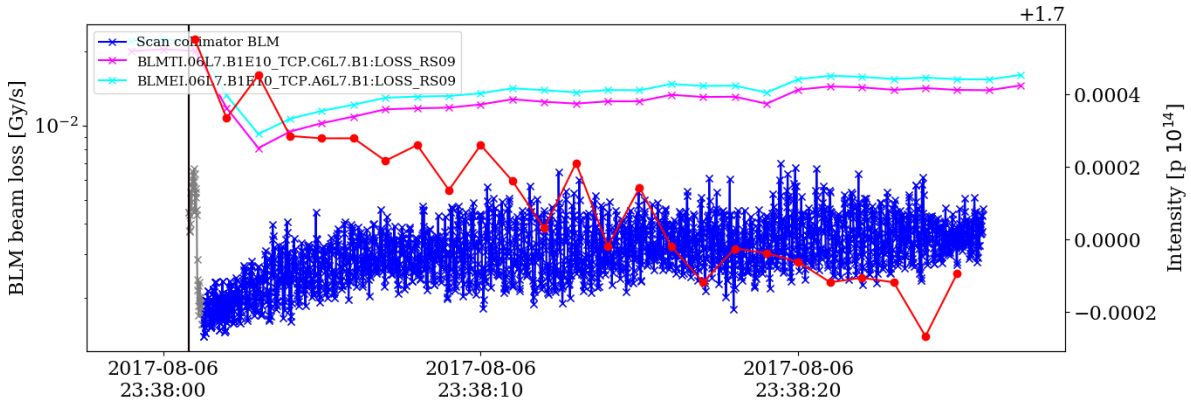

(b) Outward step

Figure 3: Examples of the one-step (top-inward, bottom-outward) data for the three primary collimators that are used in *Scenario 1, 2, and 3* (see Section 3). The loss signal from the scanning collimator is acquired at 100 Hz, while from the others are at 1 Hz. The BCTDC signal (red) is acquired at 1 Hz, clearly showing its limited resolution.

3 Analysis methodology

While the BCTDC has not enough sensitivity (see Fig. 3), the BLM system has a sufficient dynamic range to measure the losses observed during each collimator step. The BLM signal can then be calibrated w.r.t. the BCTDC one to obtain the number of lost protons per second from the measured dose in Gy/s through a proper conversion factor F expressed in protons/Gy [7]. Figure 4 illustrates the principle used for the calculation of F. The actual integrated intensity lost due to the collimator step is calculated according to $\Delta I = F\Lambda$, i.e. assuming a linear relationship, where Λ is the integrated BLM signal in Gy. The conversion factor for a given collimator jaw step is defined as

$$F = \Delta I_{\text{tot}}/\Lambda_{\text{tot}} \qquad [\text{p/Gy}]\,, \tag{1}$$

where Λ_{tot} is the integrated BLM step loss and ΔI_{tot} the corresponding absolute intensity lost recorded during the same step. The final contribution to the total beam loss is expressed as:

$$\Lambda_{\text{tot}} = \frac{w_1 \int_{\text{collscan}} + w_2 \int_{\text{coll}_2} + w_3 \int_{\text{coll}_3}}{w_1 + w_2 + w_3}\,, \tag{2}$$

where $\int_{\text{coll}}$ is the integrated loss measured by the BLM attached to a collimator that is not part of the scan, whereas $\int_{\text{collscan}}$ stands for the BLM loss at the scanning collimator. The weight w_1 of the

primary scraping collimator is always set to unity, while w_2 and w_3 vary depending on the scenario (see below).

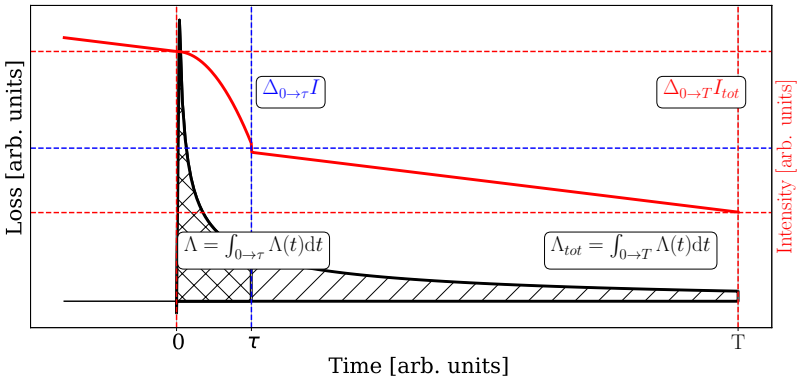

Figure 4: Illustrative sketch of the algorithm used to calculate the intensity lost (ΔI) due to the movement of the jaw that occurred in the interval $[0, \tau]$, using the total loss (Λ_{tot}) in the decay phase, i.e. the integral over the interval $[0, T]$ where T is the length of the step.

In general, the conversion factor F depends on the position of the collimator jaw relative to the beam. For the analysis described in [3], this dependence was neglected and the constant average conversion factor (see *Scenario 1*, later in the text) was used. However, a follow-up of this analysis triggered a discussion on how to improve this algorithm. The complete list of *Scenarios* considered to obtain the conversion factor is:

1. an average value between all recorded losses measured during the amplitude scan, later referred to as *Scenario 1*;

2. an amplitude-dependent value based on the losses recorded on one single BLM, namely that closest to the moving collimator ($w_1 = 1$, $w_2 = 0$ and $w_3 = 0$ in Eq. (2)), later referred to as *Scenario 2*;

3. an amplitude-dependent value based not only on the estimate from the primary scanning collimator loss monitor (collecting most of the primary losses), but also including the other primary collimators, i.e. the orthogonal plane and the skew unit. This scenario is then split in two sub-scenarios, which differ by the weights used in Eq. (2). For *Scenario 3.1* the weights have been chosen as: $w_1 = 1$, $w_2 = 0.5$ and $w_3 = 0.1$; and for *Scenario 3.2* they have been chosen as: $w_1 = 1$, $w_2 = 0.1$ and $w_3 = 0.1$. Note that while *Scenario 3.2* features realistic weights, i.e. in which the contribution to beam losses from the non-scanning collimators is only a small fraction of the total losses, *Scenario 3.1* is much more extreme, assuming that a non-scanning collimator can contribute to the beam losses up to a factor one-half of the main contribution.

During normal operation due to cross-talk, secondary showers, etc. (see the considerations in [8, 9]) to distinguish the primary protons and other losses measured by the downstream monitor, we took the liberty to probe different weights based on a guess. Here, we decided to check one extreme case (*Scenario 3.1*) and one that could potentially be more realistic (*Scenario 3.2*). A detailed reconstruction could be repeated if in the future a detailed decomposition of the losses could be established.

4 Results

To quantify the impact of the different scenarios, we have calculated three families of conversion factors. Figure 5 shows their values computed from the data of the test with the full physics beams (example fills 6052 and 7221) and MD beams, with lower intensity fills (6194 and 7392).

The data obtained from the analysis outlined earlier are shown in Fig. 7, together with a linear fit expressing the calibration function as a linear function of the transverse amplitude. The obtained fit parameters are reported in Table 1 for the various fills considered and the different scenarios.

Table 1: Summary of the fit parameters of the function $F = m\,\sigma_{\mathrm{N}} + q$ for the various scenarios and fills. All figures are expressed in units of Gy/p. n_{b} represents the total number of bunches.

Fill	n_{b}	*Scenario 1*		*Scenario 2*			*Scenario 3.1*			*Scenario 3.2*		
		m	q	m	q	R^2	m	q	R^2	m	q	R^2
		10^{-15}	10^{-13}	10^{-15}	10^{-13}	10^{-26}	10^{-15}	10^{-13}	10^{-26}	10^{-15}	10^{-13}	10^{-26}
6052	2550	NA	1.5	−92	5.8	3.0	−82	5.2	2.7	−97	6.2	3.5
6052 out		NA	0.23	−89	4.3	3.0	-	-	-	-	-	-
6194	224	NA	1.6	−54	3.8	0.7	−52	3.6	0.6	−59	4.1	0.8
7221	2550	NA	0.8	−0.45	2.5	0.01	−7.9	3.1	0.1	−3.4	2.8	0.2
7392	300	NA	0.8	−0.99	4.0	0.07	−21	5.4	0.2	−10	5.3	0.4

The plots show a good agreement between the various calibration lines, computed for the various scenarios under consideration, up to about 4σ. We might speculate that the beam profile is rather reproducible up to this amplitude, while beyond this value the profile tails are less reproducible from fill to fill, and the differences of the reconstructed losses are clearly visible. The conversion factor F computed using *Scenario 1* provides different results with respect to the others that are, in general, rather close between them. Moreover, we observe that the discrepancy persists down to amplitudes of 4.5 σ, while below that amplitude all scenarios provide very comparable results.

In Fig. 7, the comparison between the converted experimental data using various factors F for the case of Fill 6052 is shown.

5 Conclusions and outlook

In this note, we showed a summary of different approaches that can be used to reconstruct the conversion factor F, used to express the loss in p/s for collimator scans. Three approaches have been presented; two of them take into account the dependence on the amplitude of F, and one represents an amplitude-independent average. The methods including the amplitude dependence introduce a change in the background level of the losses, visible at the outer positions of the scan. We showed that including the losses on the collimators that are not used in the scan introduces further differences with respect to the standard approach. However, the difference generated by the assumptions made on the weight used for the reconstruction of the beam losses is smaller, indicating that the details of the weights, as long as they are reasonable, are not essential. In any case, the rough estimates of the weights used for the reconstruction of the calibration factor F would need to be refined, possibly with further studies on loss decomposition, e.g. primary and secondary losses w.r.t. the primary collimators measurements. These considerations might lead to more accurate estimates of the conversion factor.

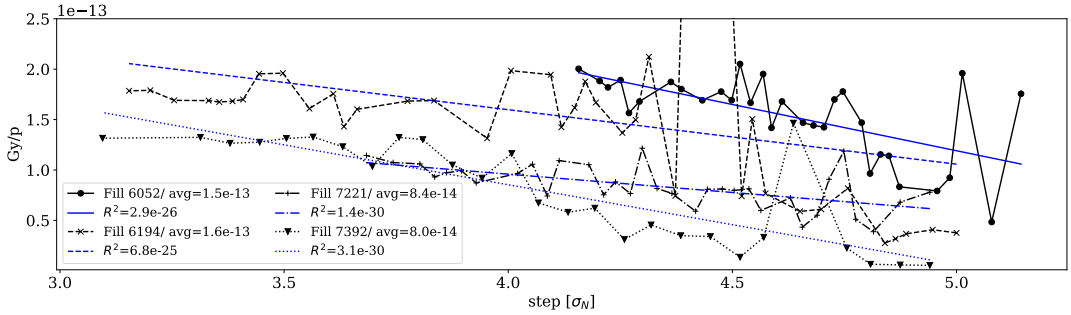

(a) *Scenario 2*: w_1=1, w_2=0, w_3=0

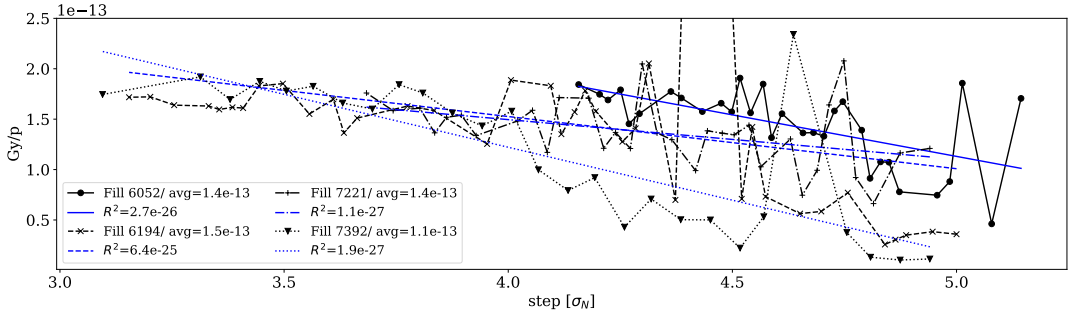

(b) *Scenario 3.1*: w_1=1, w_2=0.5, w_3=0.1

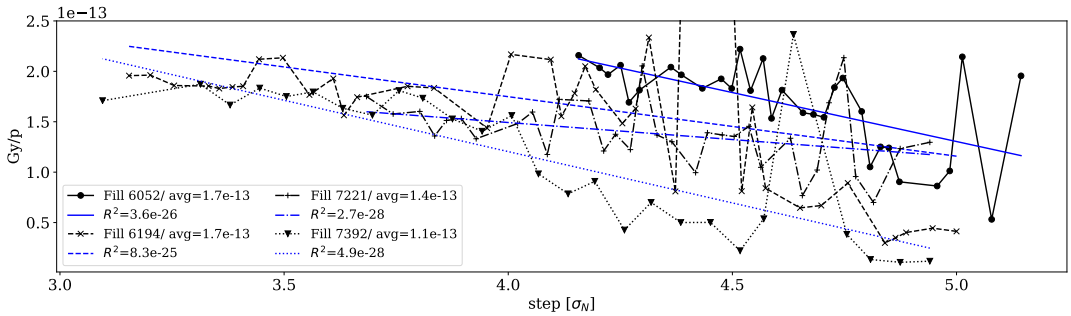

(c) *Scenario 3.2*: w_1=1, w_2=0.1, w_3=0.1

Figure 5: Results of the calculation of the conversion factor F at different scan steps (black). The average value (for a given calculation method), with approach as in *Scenario 1* is provided, together with the amplitude-dependent values for the approaches *Scenario 2, 3.1 and 3.2* as outlined in Section 3 (σ_N is calculated using the nominal emittance value of 3.5 µm).

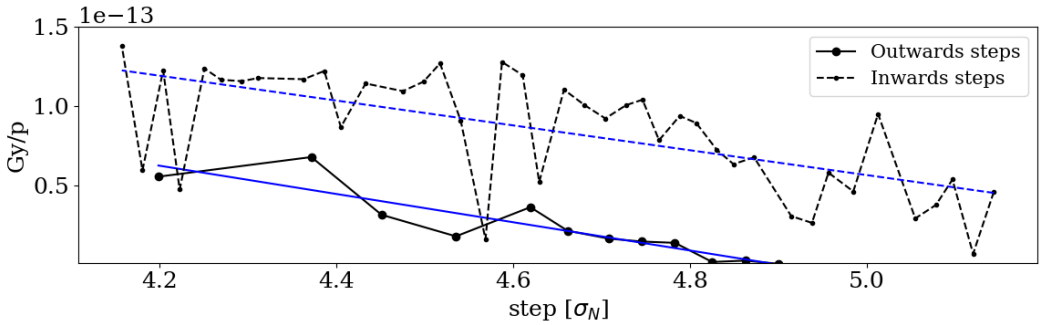

Figure 6: Results of the calculation of the conversion factor F in different scan steps (black points), inward and outward during a fill (6052). In blue is the fit value with losses calculated as in *Scenario 2* (σ_N is calculated using the nominal emittance value of 3.5 µm).

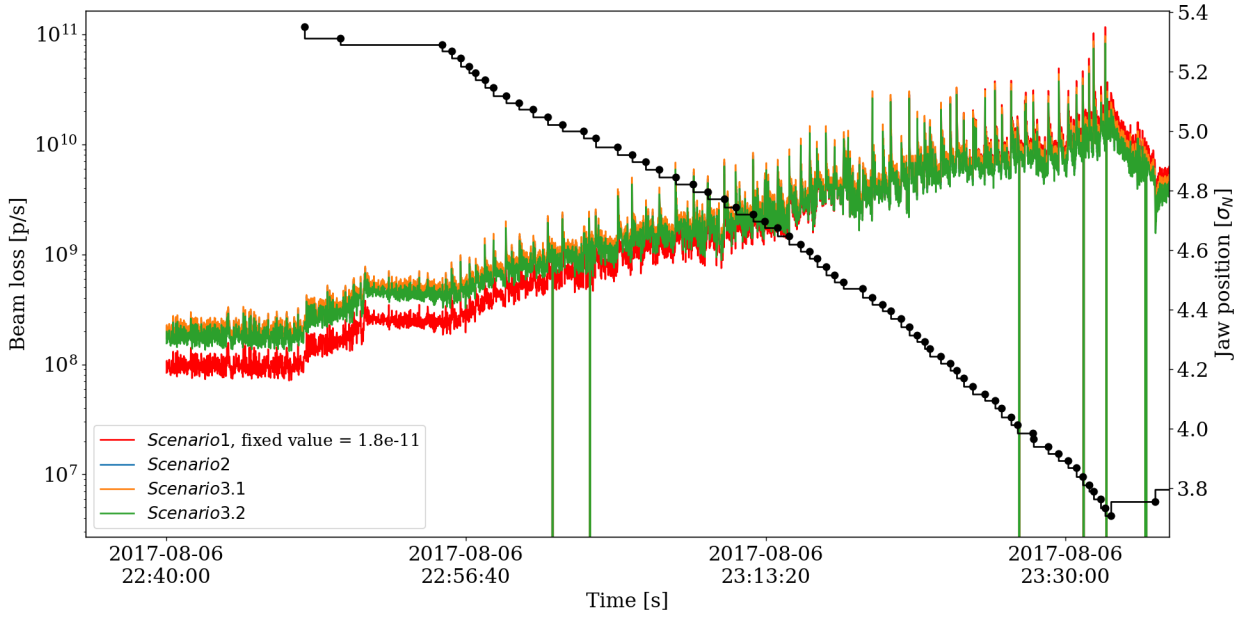

Figure 7: The beam loss along the scraping expressed in p/s (instead of the original unit Gy/s) for different approaches in obtaining the conversion factor F for Fill 6052.

A LHC Fills details

Table 2: Summary of the selected measurements performed at 6.5 TeV [3], where I_{st} is the total intensity at the start of the scraping, I_s is the total intensity lost during scraping (including luminosity burn-off) also expressed as relative loss with respect to I_{st}. σ_s is the scraped range in terms of nominal beam sigma starting from 5σ.

Fill	Date	n_b	Beam 1				Beam 2				Scans performed	
			I_{st} [10^{13} p]	I_s [10^{13} p]	%	σ_s	I_{st} [10^{13} p]	I_s [10^{13} p]	%	σ_s	Beam	Plane
6052	2017-08-06	2550	19.0	2.30	12	1.2	21.0	2.30	11	1.3	B1/B2	H/V
6194	2017-09-13	224	2.7	1.10	40	1.8	2.7	1.02	36	1.9	B1/B2	H/V
7221	2018-09-26	2550	12.0	0.65	5	1.2	15.1	0.34	2	1.2	B1/B2	V
7392	2018-10-30	300	2.1	0.23	9	1.2	2.4	0.28	10	1.2	B1/B2	H/V

B Influence of the Running Sum on the integration and fit results

The loss data used in the analysis are the so-called running sum. Figure 8 shows the difference between the different running sums. In the analysis we neglect the fact that the difference between the actual loss and the RS06 is about 1%. Moreover, it is worth noting that, when comparing between RS06 and RS09 this difference is larger (13%). As the RS09 loss signals are used only with arbitrary taken weights, we also do not apply any correction for that and account for the change in the weighted value.

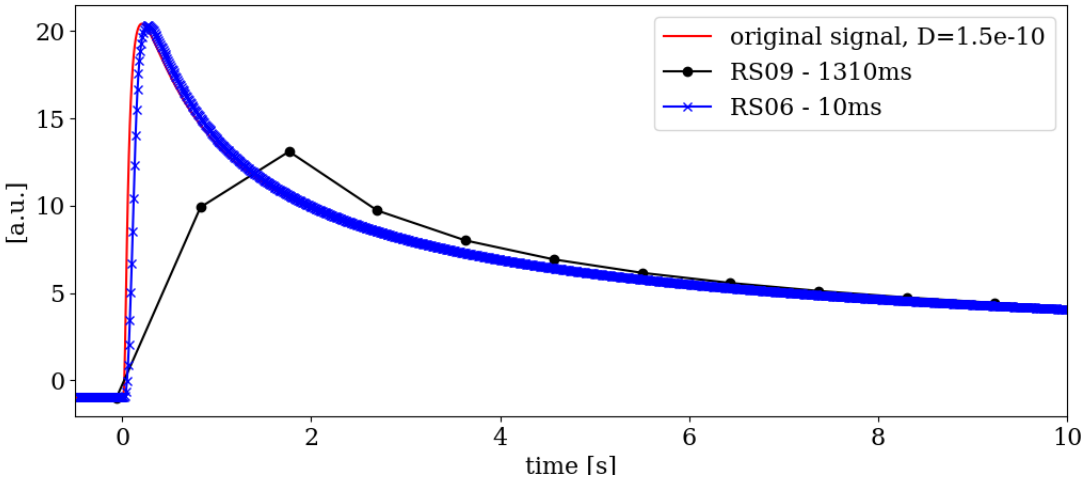

Figure 8: The evolution of actual losses (red) and processed with different running sums: RS06 at 100 Hz (blue) and RS09 at 1 Hz (black).

References

[1] O. S. Brüning et al. *LHC Design Report*. CERN Yellow Rep. Monogr. Geneva: CERN, 2004. DOI: 10.5170/CERN-2004-003-V-1.

[2] URL: https://ab-div-bdi-bl-blm.web.cern.ch/Acquisition_system/Data_acquisition_integration_durations_20100313.htm.

[3] A. Gorzawski et al. "Probing LHC halo dynamics using collimator loss rates at 6.5 TeV". In: *Phys. Rev. Accel. Beams* 23 (4 2020), p. 044802. DOI: 10.1103/PhysRevAccelBeams.23.044802. URL: https://link.aps.org/doi/10.1103/PhysRevAccelBeams.23.044802.

[4] C Roderick et al. *The LHC Logging Service : Handling terabytes of on-line data*. Tech. rep. CERN-ATS-2009-099. Geneva: CERN, 2009. URL: https://cds.cern.ch/record/1215574.

[5] G. Azzopardi, G. Valentino, and B. M. Salvachua Ferrando. "MD3343 - Fully-Automatic Parallel Collimation Alignment using Machine Learning ". In: (2018). URL: https://cds.cern.ch/record/2647213.

[6] URL: /nfs/cs-ccr-nfs99/data/LHCCollimators/fastdata/IC/.

[7] B Salvachua et al. "Lifetime Analysis at High Intensity Colliders Applied to the LHC". In: CERN-ACC-2013-0072 (2013), 3 p. URL: https://cds.cern.ch/record/1574586.

[8] G. Azzopardi, G. Valentino, and B. M. Salvachua Ferrando. "MD1653 - Part 1: Characterisation of BLM Response at Collimators". In: (2018). URL: https://cds.cern.ch/record/2647198.

[9] G. Azzopardi, B. Salvachua, and G. Valentino. "Data-driven cross-talk modeling of beam losses in LHC collimators". In: *Phys. Rev. Accel. Beams* 22 (8 2019), p. 083002. DOI: 10.1103/PhysRevAccelBeams.22.083002. URL: https://link.aps.org/doi/10.1103/PhysRevAccelBeams.22.083002.